PAPER

Effect of the amino acid composition of cyclic peptides on their self-assembly in lipid bilayers†

Maarten Danial,[a] Sébastien Perrier*‡[a] and Katrina A. Jolliffe*[b]

The effect of amino acid composition on the formation of transmembrane channels in lipid bilayers upon self-assembly of alt-(L,D)-α-cyclic octapeptides has been investigated. Cyclic peptides comprising D-leucine, alternating with different combinations of L-azidolysine, L-lysine(Alloc), L-lysine and L-tryptophan were synthesized and the size of pores formed *via* self-assembly of these molecules in lipid bilayers was elucidated using large unilamellar vesicle fluorescence assays and dynamic light scattering. Pore formation was examined in large unilamellar vesicles made up of egg yolk phosphatidylcholine or *Escherichia coli* total lipid extract. From these analyses, we have established that cyclic peptides with charged side chains form large pores while those with neutral side chains form unimeric pores. Furthermore, the cyclic peptides that consist of non-symmetric amino acid configurations possess a higher membrane activity than the cyclic peptides with a symmetric amino acid configuration. In addition, we have found that peptide amphiphilicity plays a vital role in selective partitioning between bilayers that consist of egg yolk phosphatidylcholine and those comprised of *E. coli* total lipid extract. These results suggest that selective transbilayer channel formation *via* self-assembly may be a viable alternative for many applications that currently use more expensive, multistep synthesis methods.

Introduction

Protein channels represent one class of structures that maintain cell vitality through sustaining equilibria of ions, water, pH and solutes in organelles and cells. Several prominent examples of protein channels include the aquaporins,[1,2] sodium and potassium channels,[3] chloride channels,[4] and pathogen-derived α-hemolysin.[5] These channels provide a direct route of access in which ions and water are transported efficiently across otherwise impermeable phospholipid bilayer membranes.[6] The plethora of protein channels in nature also provides inspiration for the design of drug delivery routes,[7] sequencing applications,[8] or in sensing technologies[7,9,10] providing direct access across the phospholipid bilayer membrane. While synthesis of these protein channels is feasible through biotechnological processes, adaptability and modulation of properties such as channel cavity size and ion selecti-

vity to suit different applications poses a formidable challenge. The self-assembly process to build hierarchical, supramolecular structures *via* a bottom-up approach, however, provides an alternative route that permits access to application-tailored artificial channels. In addition, the self-assembly process also avoids low-yielding, multistep synthesis procedures to create functional structures thereby lowering the cost, increasing the ease of production and ultimately making self-assembled transmembrane channels desirable for use in a range of the aforementioned applications.

Artificial transmembrane channels have been created *via* self-assembly from crown-ethers,[11] peptides,[12,13] oligoamides,[14] nucleotides,[15,16] cyclodextrins,[17,18] and aromatic macrocycles.[19–21] Features of these and other artificial transmembrane channels including ion transport selectivity as well as specificity have been reviewed recently.[22–24] Additionally, some remarkable examples of solute-specific transport using self-assembled structures have also been reported. Liu *et al.* reported a light-responsive ion channel based on a benzo-crown ether bound to an azobenzene group with an dodecyl aliphatic tail.[25] Upon adoption of the *cis* conformation with 365 nm UV light, the benzocrown ethers stacked to form a 2.8 Å channel, which had an increased affinity with the lipid bilayer compared to the *trans*-ion channel, thereby showing that stimuli responsive ion-specific channels can be created. In another example, Langecker *et al.* constructed a 2 nm artificial channel through the molecular self-assembly of a double

[a]Key Centre for Polymers & Colloids, The University of Sydney, School of Chemistry, Building F11, Sydney NSW 2006, Australia. E-mail: S.Perrier@warwick.ac.uk
[b]The University of Sydney, School of Chemistry, Building F11, Sydney NSW 2006, Australia. E-mail: Kate.Jolliffe@sydney.edu.au

stranded DNA stem with cholesterol-modified single stranded DNA to form a cap and mediate lipid attachment.[15] Single molecule translocation experiments showed that these artificial channels were able to discriminate single DNA molecules.

Cyclic peptides that self-assemble into nanotubular structures have also offered a versatile route to create artificial channels.[26,27] This is in part due to employing high yielding solid phase peptide synthesis methods, which provides access to large amounts of material. Furthermore, through modifying the length of the peptide, precise molecular control over channel diameter can be achieved making it a viable route to create channels with different diameters. Cyclic peptides that contain alternating α-D,L amino acids have therefore been an attractive template to form well-defined nanotubes and channels with cavity diameters ranging from 2 to 13 Å.[13,28–32] Another appealing feature of these self-assembling cyclic peptides is that the alternating absolute configuration projects the amino acid side chains out of the plane of the cyclic peptide and enables chemical modification of the peptide side chains without causing significant interference with the extensive hydrogen bonding perpendicular to the plane of the cyclic peptide.

Functionalization of the cyclic peptide side chains with (macro)molecules and the effect upon the properties of nanotubes[33–38] and artificial channels[39–41] is an exciting recent development of these systems. Although, the effect of the amino acid configuration and type of peptide side chains upon artificial channel formation has been studied,[13,27–30,39,42–44] only a selection of studies have investigated the lipid bilayer partitioning of self-assembling cyclic peptides that contain non-natural β- or γ-amino acids.[45,46] To the best of our knowledge, no previous study conducted has described the effects on lipid bilayer partitioning of octameric cyclic peptides that contain non-natural α-L-amino acids.

In this paper we investigate the effect upon lipid bilayer channel formation of six different cyclic peptides that are comprised of natural and non-natural α-L amino acids or have amino acid configurations that have not previously been examined. The type of pore formed was elucidated via dynamic light scattering and two independent, pore-size-discriminating large unilamellar vesicle assays, which either had calcein or 5(6)-carboxyfluorescein entrapped. Furthermore, the concentration-dependent pore-formation is examined for two types of LUVs, consisting of Egg yolk phosphatidylcholine (EggPC) and *Escherichia coli* total lipid extract, respectively.
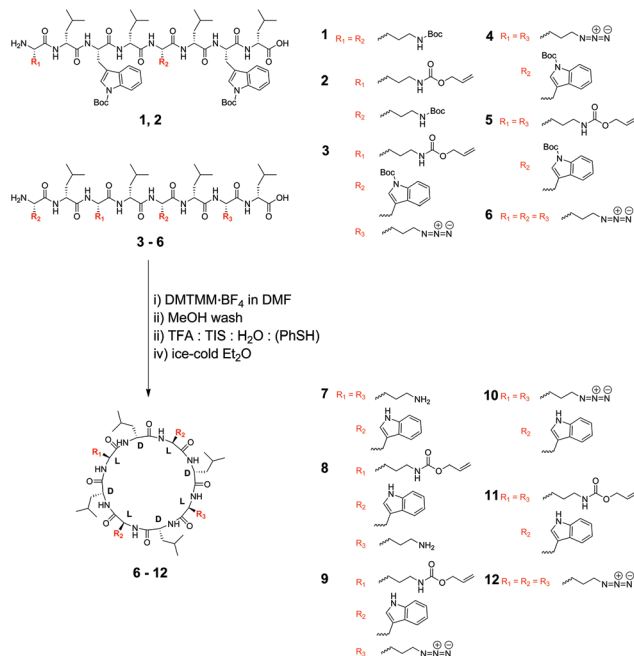
Results and discussion

Synthesis

Cyclic peptides that consist of alternating L- and D-α-amino acids have previously been shown to adopt a low-energy, flat ring conformation that self-assembles into nanotubes in solution[47,48] as well as in lipid bilayers.[13,30] Although studies have explored variations in the type of cyclic peptide on phospholipid channel formation, only a limited number of variations

in amino acid constituents have been investigated (for a recent review refer to Montenegro *et al.*[27]). For instance, Ghadiri *et al.* noted that octameric cyclic peptides that consisted only of L-glutamine and D-leucine did not have the appropriate surface characteristics to partition into lipid bilayers.[13] Furthermore, additional studies predominantly explored application of cyclic peptides that contain α-D,L-amino acids,[13,30,39,43,44] β-amino acids[45] or γ-amino acids.[46] We chose to use cyclic peptides comprising eight α-amino acids as opposed to analogs with four, six or ten residues or β-/γ-amino acids for several reasons. Firstly, cyclic peptides with eight amino acid residues can easily be synthesized to high purity from commercially available or readily accessible starting materials without requiring reverse phase purification protocols. Secondly, cyclic peptides comprising six amino acids or less possess small cavity sizes (<0.6 nm) through which limited solute transport may be observed. Thirdly, based on experiments using *N*-alkylated cyclic peptides, the tetrameric, hexameric and decameric analogues exhibit lower association constants than the octameric systems, suggesting stronger self-assembly into nanotubes for the cyclic octapeptides.[26] In this work, we therefore investigated the ability to form lipid bilayer pores by self-assembly of octameric cyclic peptides. These cyclic peptides consisted of natural and non-natural amino acids, with the number of leucine residues held constant, while the alternating side chains were varied to allow an investigation of side chain functionality on membrane partitioning. Cyclic peptides (**7–11**) included two L-tryptophan residues, which had previously been shown to be required for bilayer partitioning,[13] while cyclic peptide **12**, which excluded tryptophan, was synthesized to establish whether the L-azidolysine side chain was capable of promoting phospholipid bilayer partitioning and channel formation in the absence of Trp. A combination of lysine-derived charged (amine, -NH$_3^+$), polarizable (azido, -N$_3$), and allyloxycarbonyl (-Alloc) side chains were employed to establish the role of these different functionalities on membrane partitioning, without varying the distance of the functional group from the peptide core or significantly altering the size of the side chains. Cyclic peptides **8** and **9** were unsymmetrically substituted by positioning different side chains on opposite sides of the peptide core to establish whether this resulted in changes to membrane partitioning. In addition and for the first time, the role of these amino acid side chains on channel formation in phospholipid bilayers made from zwitterionic EggPC or negatively charged *E. coli* total lipid extract was investigated.

Synthesis of the required linear peptide precursors (**1–6**) was achieved through solid phase peptide synthesis[49] followed by mild, selective cleavage from a chlorotrityl chloride resin using 20% hexafluoroisopropanol in dichloromethane (Scheme 1) without deprotection of the Boc groups. Although the sequence of amino acids within the linear peptide chain was varied to terminate with L-lysine (**1** and **2**), with L-tryptophan (**3–5**) or with L-azidolysine (**6**) at the N-terminus, this difference did not influence the overall linear peptide synthesis yields or purity. Subsequently, cyclization of the

This journal is © The Royal Society of Chemistry 2015

Org. Biomol. Chem., 2015, **13**, 2464–2473 | **2465**

Scheme 1 Synthesis of cyclic peptides used in this study.

Fig. 1 Illustration showing the different possible modes of bilayer channel formation. Formation of cyclic peptide channels in a lipid bilayer can occur as (a) a unimeric pore, (b) a barrel stave or (c) through a bilayer (carpet-like) disruption.

Boc-protected linear peptide precursors was achieved under high dilution *via* addition of a 4-(4,6-dimethoxy-1,3,5-triazin-2-yl)-4-methylmorpholinium tetrafluoroborate (DMTMM·BF$_4$) reagent (Scheme 1). The DMTMM·BF$_4$ reagent has been shown to be an effective coupling agent that can improve cyclization yields[50] and can be produced at high synthesis scales.[51]

The structure of the cyclic peptides was verified by MALDI-FTICR mass spectrometry as well as NMR spectroscopy. Specifically, the disappearance of the signals attributable to the N-terminal α-CH at ~4.4 ppm and the C-terminal α-CH at ~4.7 ppm, respectively confirmed cyclization for the peptides terminating with lysine derivatives **1**, **2** and **6**. Similarly, cyclization of the peptides **3–5**, which have N-terminal tryptophan (Boc) was confirmed by the disappearance of the signals attributable to the N-terminal α-CH and C-terminal α-CH at ~4.1 ppm and ~4.7 ppm, respectively. As shown previously,[41] cyclization of the linear peptides can also be determined using distortionless enhancement by polarization transfer-edited heteronuclear single quantum coherence (HSQC) NMR spectroscopy (Fig. S1–S6†). In addition, the tendency of the cyclic peptides to aggregate, in contrast to the linear peptide precursors, was confirmed by dynamic light scattering.

Characterization of pore type

The structure of the phospholipid bilayer channel formed was characterized using pore-size-discriminating large unilamellar vesicle (LUV) assays along with dynamic light scattering (DLS) analysis. As shown in Fig. 1, the main modes of transbilayer channel formation are *via* unimeric pores, barrel staves and bilayer (carpet-like) disruption.[52] To assess which transbilayer channels are formed, LUVs with either calcein or 5(6)-carboxy-fluorescein entrapped w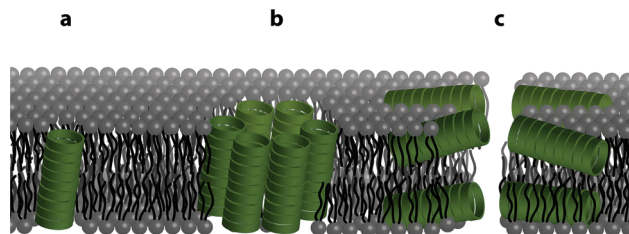ere prepared. The formation of barrel staves or lipid bilayer disruption as depicted in Fig. 1b and c was assayed with the calcein-entrapped LUVs. Calcein serves as a reporter fluorescent dye (average diameter ~ 1.5 nm), which is self-quenched at high concentrations and upon dilution (<8 μM) results in a fluorescence band maximum at 505 nm (ESI Fig. S7†). Molecular confinement of calcein within the lumen in the LUVs leads to self-quenching while release *via* barrel staves or lipid bilayer disruption causes a reduction in calcein self-quenching. In addition to this assay, dynamic light scattering was performed to exclude the possibility of LUV lysis as a result of lipid bilayer disruption within the time-frame of the LUV assay, thereby corroborating the formation of barrel staves. The presence of smaller pores, *e.g.* unimeric pores (channel diameter < 0.8 nm) as depicted in Fig. 1a, was revealed with LUVs that contained the pH responsive fluorescent dye 5(6)-carboxyfluorescein, which has a weak fluorescence emission in acidic pH and a strong fluorescence emission at pH > 7. The formation of unimeric pores upon the addition of the cyclic peptides was established using LUV assays with a pH gradient across the phospholipid bilayer, in which the internal LUV environment consisted of a phosphate buffer at pH 5.8 and the external environment consisted of a phosphate buffer at pH 7.4. Collapse of the transbilayer pH gradient due to the formation of transbilayer channels causes an efflux of protons and thus neutralizes the internal LUV environment and results in an increase in 5(6)-carboxyfluorescein fluorescence emission.

Dynamic light scattering experiments of the LUVs were employed to assess the integrity of the lipid bilayer upon the addition of the cyclic peptides. Upon the formation of unimeric pores and barrel staves, LUV integrity should remain stable unless a high osmotic difference between the internal and external environment causes breakdown of the LUV lipid bilayer. Thus in all experiments, no osmotic potentials across lipid bilayers were introduced. Conversely, lipid bilayer disruption and breakdown of the LUVs into smaller aggregates should be evidenced by DLS by a distribution shift to smaller hydrodynamic radius. As a control, triton X-100 was added to LUVs in order to assess the changes in the hydrodynamic radius distribution upon LUV lysis and hence loss of lipid bilayer integrity.

The cyclic peptides were examined for their lipid bilayer partitioning and their propensity to form barrel staves or

Fig. 2 (a) Calcein dye leakage experiments with EggPC LUVs upon addition of cyclic peptides (final concentration = 19 μM) at approximately 60 seconds. The fraction of calcein fluorescence measured is relative to 100% LUV lysis in the presence of triton X-100. (b) Dynamic light scattering (CONTIN) hydrodynamic radius (R_H) distributions obtained with EggPC LUVs upon the addition of cyclic peptides or triton X-100.

bilayer disruption using calcein-entrapped LUVs made from egg yolk phosphatidylcholine (EggPC) or made from *E. coli* total lipid extract. As presented in Fig. 2a, the addition of cyclic peptides 7 and **8**, which contain the positively charged lysine residues, to LUVs prepared from EggPC resulted in immediate calcein release and fluorescence increases of 80% and 65%, respectively, after 200 s. In contrast, little to no change in fluorescence was observed upon the addition of cyclic peptides **9–12** to EggPC LUVs containing calcein. Furthermore as shown in Fig. 2b, hydrodynamic radius (R_H) distributions of the LUV solutions centered at ~55 nm obtained from dynamic light scattering indicated that, within the timeframe of the experiment, LUV lysis did not result upon the addition of cyclic peptides **7–12**. The size distribution profile upon the addition of cyclic peptide **10**, however, revealed an additional species that was attributed to the formation of large aggregates (R_H ~ 200–300 nm) caused by limited solubility of

this cyclic peptide in aqueous buffer (Fig. 2b). Further corroboration for the formation of barrel staves as opposed to bilayer disruption due to the addition of cyclic peptides was achieved *via* concentration dependent measurements (*vide infra*) as well as comparison to LUV lysis through the addition triton X-100, which leads to a hydrodynamic radius centered at 3–4 nm (Fig. 2b). Taken together, these results strongly suggest that the cause for calcein dye leakage from the LUVs upon the addition of cyclic peptides 7 and **8**, both of which have positively charged side chains, results from the formation of barrel staves rather than *via* bilayer disruption.

Similarly, LUVs prepared from *E. coli* total lipid extract also showed release of calcein upon addition of cyclic peptides 7 and **8**, albeit only leading to a fluorescence increase of 6% and 40%, respectively (Fig. 3a). Notably, the asymmetric amphiphilic cyclic peptide **8**, which contains ʟ-Lysine and ʟ-Lysine(Alloc)
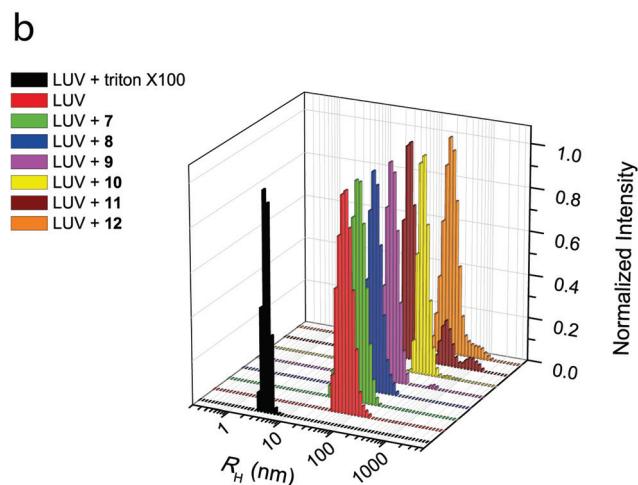

Fig. 3 (a) Calcein dye leakage experiments with LUVs made from *E. coli* total lipid extract upon addition of cyclic peptides (final concentration = 19 μM) at approximately 60 seconds. The fraction of calcein fluorescence measured is relative to 100% LUV lysis in the presence of triton X-100. (b) Dynamic light scattering (CONTIN) hydrodynamic radius (R_H) distributions obtained with *E. coli* LUVs upon the addition of cyclic peptides or triton X-100.

This journal is © The Royal Society of Chemistry 2015

Org. Biomol. Chem., 2015, **13**, 2464–2473 | **2467**

residues on opposite sides of the cyclic peptide ring caused a higher calcein dye release from the LUV than the symmetric cyclic peptide **7**, which contains two L-Lysine residues. As shown in Fig. 3b, dynamic light scattering confirmed that the LUVs remained intact in the presence of the cyclic peptides suggesting that bilayer disruption and LUV lysis was not the cause of calcein release. Further evidence that rules out the formation of carpet-like bilayer disruptions was evident from concentration dependent experiments with 5(6)-carboxyfluorescein entrapped LUVs (*vide infra*). Similar to experiments performed with EggPC LUVs, dynamic light scattering revealed large aggregates ($R_H \sim 200–300$ nm) in mixtures of the LUVs and cyclic peptides **10** and **12**. These aggregates were attributed to the limited solubility of cyclic peptides **10** and **12** in aqueous solution but also suggested that minimal phospholipid bilayer partitioning was taking place in the form of unimeric pores.

The formation of large pores in both calcein-entrapped LUVs composed of EggPC and *E. coli* total lipid extract was also evident in the assay with 5(6)-carboxyfluorescein entrapped LUVs. As Fig. 4 shows, the highest fluorescence response was due to cyclic peptide **7** and **8** whereby the activity difference between LUVs made from EggPC or *E. coli* total lipid extract was consistent with observations made in the calcein-entrapped LUV assays (*vide supra*). In contrast to the experiments with calcein-entrapped LUVs, the addition of cyclic peptides **9–12** to LUVs containing 5(6)-carboxyfluorescein resulted in a 20–40% fluorescence increase in EggPC LUVs and a 10–35% fluorescence increase in LUVs made from *E. coli* total lipid extract. Notably, a higher degree of unimeric pore formation was evident with cyclic peptide **9** compared to cyclic peptides **10–12**. Once again, asymmetry within cyclic peptide **9** with a single L-azidolysine opposite a single L-lysine (Alloc) may promote the lipid bilayer partition activity over symmetric cyclic peptides **10–12**, which do not possess two different amino acids opposite each other in the cyclic peptide ring. A slight difference between cyclic peptide induced pore formation in LUVs made from EggPC and *E. coli* total lipid extract was observed (Fig. 4). The lower degree of pore formation of cyclic peptide **12** in LUVs made from *E. coli* total lipid extract agrees with a higher degree of aggregation observed by DLS measurements (Fig. 3b). The low degree of pore formation in both types of LUVs upon the addition of cyclic peptide **12**, which lacks tryptophan residues, was consistent with previous studies in which L-tryptophan was replaced with L-glutamine.[13]

Concentration dependence on pore formation

A concentration titration of the cyclic peptides was performed on LUVs made from EggPC and *E. coli* total lipid extract to establish the concentration-dependent pore-formation activity as well as support previous experiments that provide information for barrel stave formation over carpet-like bilayer disruption. As Fig. 5 shows, an increase in concentration of the cyclic peptide corresponded to a non-linear increase in fluorescence emission upon incubation with 5(6)-carboxyfluores-
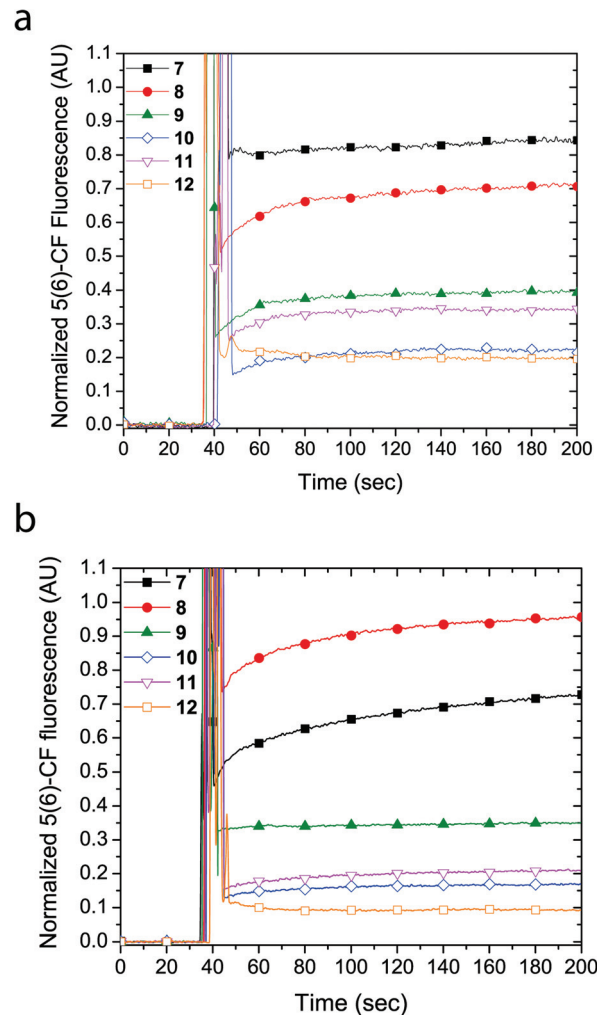

Fig. 4 Proton efflux measured using 5(6)-carboxyfluorescein entrapped in LUVs made from (a) EggPC or (b) *E. coli* total lipid extract. The cyclic peptide was added to the LUV mixture ~ 40 seconds (final concentration = 19 μM). The fluorescence signal is normalized against 100% LUV lysis upon the addition of triton X-100.

cein-entrapped LUVs. While these trends reveal that the concentration of all cyclic peptides required to reach 50% proton efflux varies, the concentration-dependent fluorescence response also indicated that no 'leaky' phospholipid membranes were formed upon the addition of cyclic peptide and thus affirms the absence of phospholipid bilayer disruption. Comparison of titration results revealed a larger fluorescence transition observed with LUVs made from EggPC than with LUVs made from *E. coli* total lipid extract (Fig. 5). Although the source of these variations between LUVs composed of EggPC and LUVs composed of *E. coli* total lipid extract is still unclear, these results may have implications for antibacterial applications.

Another purpose of the titration series presented in Fig. 5 was to perform a Hill analysis,[53] which ultimately reveals the concentration of cyclic peptide required to reach 50% proton efflux (EC_{50}) as well as the Hill coefficient (*n*). However, the results obtained *via* the Hill analysis were not reliable since

2468 | *Org. Biomol. Chem.*, 2015, **13**, 2464–2473

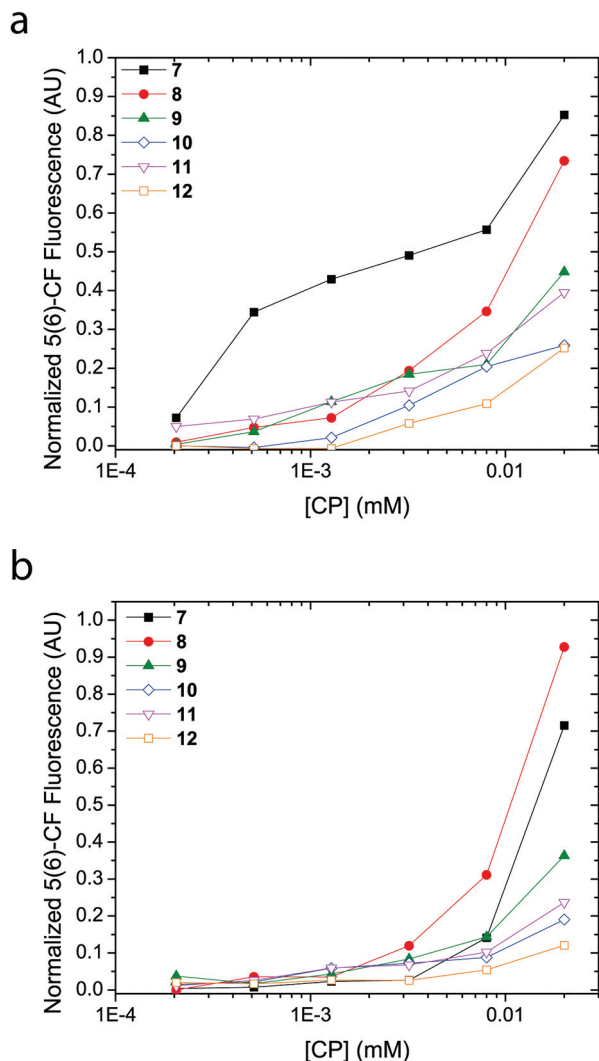This journal is © The Royal Society of Chemistry 2015

a

b

Fig. 5 5(6)-carboxyfluorescein fluorescence response as a function of cyclic peptide concentration. A non-linear concentration dependent fluorescence response indicates unimeric pore formation in 5(6)-carboxyfluorescein-entrapped LUVs made from (a) EggPC and (b) *E. coli* total lipid extract.

the majority of the cyclic peptides (9–12) did not reach 50% proton efflux within the concentration range assayed. Applying a non-linear regression modeling procedure on the data presented in Fig. 5 led to large errors so EC_{50} values and Hill coefficients could not be determined. While addition of data points at higher concentrations of cyclic peptide would remedy the error, attempts to increase the concentration of cyclic peptide in the assay while keeping the concentration of DMSO at 2 vol.% were unsuccessful and resulted in precipitation. Precipitation in the LUV assay does not provide an accurate measure for channel activity determined *via* the 5(6)-carboxyfluorescein-entrapped LUV assay because the fraction of active cyclic peptides in solution is unknown. Alternatively, an elevated concentration of cyclic peptides could also be achieved by addition of a larger aliquot to the solution containing LUVs. However, the increased DMSO content would result in a

compromised phospholipid bilayer stability and may cause contents of the LUV to leak out in to the external medium thereby influencing the result obtained by fluorescence spectroscopy. Since determination of the EC_{50} and Hill coefficient cannot be attained reliably in this contribution, information on the cooperativity, stoichiometry and stability of the transbilayer supramolecular assembly will be subject of future work.

Although membrane activity of peptides and proteins is still poorly understood, the differences observed in pore formation by cyclic peptides 7–12 (barrel stave formation by 7 and 8 and unimeric pore formation by 9–12) can be attributed to differences in how the different functional groups interact with the lipid bilayer, together with the differences in charge and intrinsic lipid curvature profiles of the EggPC and *E. coli* total lipid extract lipid components. It is expected that while the positively charged side chains of 7 and 8 might interact with the lipid headgroups, they would not interact with the hydrophobic membrane interior. This may explain the barrel-stave pores formed by these peptides in which the positively charged side chains can be effectively screened from the membrane lipids by projection into the interior of the macropores and/or towards the neighbouring 'staves'. In contrast, unimeric pores are observed for compounds 9–12, which bear side chains more likely to partition into the interior of the membrane.

Significant differences between pore formation by 7 and 8 were also observed in vesicles with differing lipid compositions. These may be a result of the differences in intrinsic curvature between EggPC and *E. coli* total lipid extract. The intrinsic curvature of a bilayer is induced by the size ratio of the lipid head group to the lipid acyl tail domain and ultimately establishes whether phospholipid bilayers are energetically stable. In phospholipid bilayers, cyclic peptides 7 and 8 could form barrel staves as illustrated in Fig. 6a and b, respectively. EggPC consists of zwitterionic phosphatidylcholine lipids (99.5%), *e.g.* 1-palmitoyl-2-oleoyl-*sn*-glycero-3-phosphocholine and a small proportion of sphingomyelin (0.5%),[54] which has been determined to possess near-zero intrinsic curvature.[55] A near-zero intrinsic curvature implies that a low energy barrier has to be overcome if the bilayer folds around the barrel stave without exposing the hydrophobic acyl domain
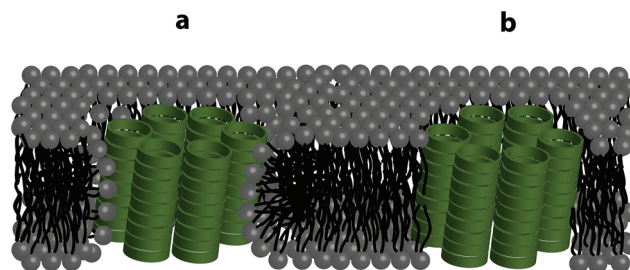

Fig. 6 Two proposed modes of barrel staves upon interaction of (a) cyclic peptide 7 with phospholipid bilayers made from EggPC, which possesses near-zero intrinsic lipid curvature and (b) cyclic peptide 8 with phospholipid bilayers made from *E. coli* total lipid extract, which has strong negative intrinsic lipid curvature.

This journal is © The Royal Society of Chemistry 2015

Org. Biomol. Chem., 2015, **13**, 2464–2473 | **2469**

to the cyclic peptide amine side chains (Fig. 6a). As a result of near-zero intrinsic curvature of EggPC bilayers, we propose that the positively charged L-lysine amine side chains of cyclic peptide **7** intercalate with the zwitterionic lipid headgroups of EggPC (Fig. 6a). Conversely, the addition of amphiphilic cyclic peptide **8** to LUVs made from EggPC suggests barrel stave formation as illustrated in Fig. 6b. This proposed structure has been suggested to be stabilized by van der Waals interactions between the acyl tail domain of the phospholipid bilayer. In this system, the L-lysine(Alloc) side chain could interact with the lipid tails leading to the projection of positively charged L-lysine side chains into the barrel stave cavity (Fig. 6b).

In contrast to EggPC, the composition of *E. coli* total lipid extract consists of zwitterionic phosphatidylethanolamine (57.5%), negatively charged phosphatidylglycerol (15.1%) and negatively charged cardiolipin (9.8%).[54] This lipid composition leads to a bilayer with strong negative intrinsic curvature[55] and would explain the low calcein release observed upon addition of cyclic peptide **7** to the LUVs as the scenario illustrated in Fig. 6a in which bilayer folding takes place to accommodate interactions with positively charged L-lysine side chains of cyclic peptide **7** is energetically unfavorable. Barrel stave formation upon addition of amphiphilic cyclic peptide **8** to bilayers made from *E. coli* total lipid extract is proposed in Fig. 6b. In this proposal, the L-lysine(Alloc) side chain on cyclic peptide **8** intercalates with the phospholipids *via* van der Waals interactions.

Conclusions

In this paper the propensity of six structurally different cyclic peptides to self-assemble into transbilayer pores in phospholipid bilayers made from egg yolk phosphatidylcholine and from *E. coli* total lipid extract was investigated. The type of transbilayer pore formed by each cyclic peptide was elucidated *via* pore-size discriminating LUV assays and dynamic light scattering of the LUVs in the presence of the cyclic peptide. The results obtained from the calcein-entrapped LUV assay indicate that cyclic peptides with amine sidechains (**7** and **8**), which would be expected to be protonated under the assay conditions (pK_a ~ 10.5), had the propensity to form larger pores than the non-charged cyclic peptides (**9–12**) in LUV bilayers. The LUV assays also revealed that symmetric cyclic peptide **7** with two amino side-chains had low activity upon incubation with LUVs made from *E. coli* total lipid extract while having the highest activity of all peptides investigated with LUVs made from egg yolk phosphatidylcholine. Conversely, asymmetric cyclic peptide **8** with only one amino side chain demonstrated higher pore forming activity in LUVs made from *E. coli* total lipid extract than observed in LUVs made from egg yolk phosphatidylcholine. This result demonstrates that the amphiphilicity of the cyclic peptide plays a pivotal role in partitioning of these molecules within bilayers made from *E. coli* total lipid extract in contrast to bilayers

made from egg yolk phosphatidylcholine. Furthermore, the 5(6)-carboxyfluorescein-entrapped LUV assays also demonstrated that incorporation of L-tryptophan and L-lysine(Alloc) residues in the cyclic peptide promote pore formation. Together, these results indicate that new combinations of amino acids within a self-assembling cyclic peptide can lead to the emergence of novel biomembrane–active materials.

Experimental

Materials

All reagents and solvents were used as received from commercial suppliers unless specifically mentioned. The cyclization coupling agent 4-(4,6-dimethoxy-(1,3,5)triazin-2-yl)-4-methyl-morpholinium tetrafluoroborate (DMTMM·BF$_4$) was prepared as described by S. A. Raw.[51] The Fmoc-protected L-azidolysine was prepared as described by Chapman *et al.*[37]

Synthesis of cyclo-[L-Lys-D-Leu-L-Trp-D-Leu]$_2$ 7. The synthesis of cyclic peptide **7** from linear peptide **1** has been described in Danial *et al.*[41] Briefly, linear peptide **1** (400 mg, 0.27 mmol) was dissolved in DMF (6 mL). To this solution, DMTMM·BF$_4$ (1.2 equiv., 105 mg, 0.32 mmol) was added and stirred for 5 days. The volume of the solution was reduced under a stream of N$_2$(g) and was precipitated in ice-cold methanol (10 mL). Yield 220 mg (56%). The Boc-protected cyclic peptide was then stirred for 3 hours in a cleavage cocktail (3 mL of TFA/H$_2$O/tri-isopropylsilane with ratio 95/2.5/2.5 vol. %) followed by precipitation and washing in ice-cold diethyl ether yielding the deprotected cyclic peptide **7** in quantitative yield. ^{1}H-NMR (500 MHz, TFA-*d*): 8.21 (d, 2H), 7.74 (d, 2H), 7.63 (s, 2H), 7.48–7.42 (m, 4H), 5.32 (t, 2H), 4.89–4.78 (m, 6H), 3.39–3.23 (overlapping m, 8H), 2.0–0.6 (m, 48 H). ^{13}C-NMR (125 MHz, TFA-*d*): 173.6, 172.0, 157.2, 135.3, 125.8, 124.0, 118.8, 116.9, 53.2, 52.6, 51.9, 42.2, 40.7, 32.7, 26.0 24.5, 21.8, 21.3, 19.9. HRMS (MALDI-FTICR) *m/z* [M + Na]$^+$: calculated: 1103.6740, found: 1103.6746. See Fig. S1† for HSQC NMR.

Synthesis of cyclo-[L-Lys(Alloc)-D-Leu-L-Trp-D-Leu-L-Lys-D-Leu-L-Trp-D-Leu] 8. The synthesis of cyclic peptide **8** from linear peptide **2** has been described in Danial *et al.*[40] Briefly, linear peptide **2** (370 mg, 0.25 mmol) was dissolved in DMF (6 mL). To this solution, DMTMM·BF$_4$ (1.2 equiv., 100 mg, 0.30 mmol) was added to the mixture and stirred for 3 days. The volume of the solution was reduced under a stream of N$_2$(g) and was precipitated and washed in ice-cold methanol (10 mL). Yield 149 mg (56%). The Boc-protected cyclic peptide was then stirred for 3 hours in a cleavage cocktail (3 mL of TFA/H$_2$O/triisopropylsilane with ratio 95/2.5/2.5 vol.%) followed by precipitation and washing in ice-cold diethyl ether yielding the deprotected cyclic peptide **8** in quantitative yield. ^{1}H-NMR (500 MHz, TFA-*d*): 8.14 (d, 2H), 7.67 (d, 2H), 7.56 (s, 2H), 7.40–7.34 (m, 4H), 5.87 (m, 1H), 5.33 (d, 1H), 5.29 (d, 1H), 5.24 (t, 2H), 4.89–4.68 (m, 8H), 3.3–3.1 (overlapping m, 8H), 2.0–0.6 (m, 48H). ^{13}C-NMR (125 MHz, TFA-*d*): 173.6, 172.0, 157.2, 135.3, 130.4, 125.8, 125.5, 124.3, 124.1, 121.9, 118.2, 117.0, 67.7, 65.9, 53.2, 52.9, 51.9, 42.1, 40.8, 32.7, 26.0,

24.5, 21.9, 21.3, 20.9, 19.9. MALDI-FTICR m/z [M + Na]$^+$: calculated: 1187.6969, found: 1187.6952. See Fig. S2† for HSQC NMR.

Synthesis of cyclo-[L-Trp-D-Leu-L-Lys(N$_3$)-D-Leu-L-Trp-D-Leu-L-Lys(Alloc)-D-Leu] 9. DMTMM·BF$_4$ (208 mg, 0.634 mmol) was added to a solution of linear peptide **3** (745 mg, 0.528 mmol) in anhydrous DMF (106 mL), c = 0.005 M. The resulting mixture was stirred at ambient temperature for 5 d after which time the DMF was removed under reduced pressure. MeOH was then added to provide a suspension, which was subsequently cooled in an ice bath and then filtered under vacuum to collect the precipitate, which was washed with cold MeOH (10 mL). The filtrate was re-concentrated under reduced pressure, suspended in MeOH and filtered, each time colleting the precipitate. This process was repeated until the filtrate was free of any precipitate. The combined precipitates were dried under high vacuum to provide the desired Boc-protected cyclic peptide (349 mg, 47%) as an off-white solid. ^{1}H NMR (400 MHz, TFA-d, with 10 equiv. LiBr) δ ppm 8.12 (d, J = 8.2 Hz, 2H), 7.63 (d, J = 7.6 Hz, 2H), 7.54 (s, 2H), 7.38 (t, J = 7.8 Hz, 2H), 7.32 (t, J = 7.2 Hz, 2H), 5.93–5.80 (m, 1H), 5.31 (d, J = 17.2 Hz, 1H), 5.25 (d, J = 10.5 Hz, 1H), 5.20 (t, J = 7.2 Hz, 2H), 5.15–5.01 (m, 1H), 4.78–4.62 (overlapping m, 7H), 3.38–3.12 (m, 8H), 1.90–1.11 (m, 24H), 0.94–0.71 (m, 24H). HRMS (ESI+) m/z [M + Na]$^+$ calculated: 1413.7905, found: 1413.7863. The Boc-protecting groups were removed by treating with TFA/triisopropylsilane/water (90 : 5 : 5 v/v/v, 3 mL) for 4 h under an atmosphere of nitrogen. The reaction mixture was afterwards concentrated under reduced pressure and then triturated with cold diethylether to give **9** as an off-white solid in quantitative yield. HRMS (MALDI-FTICR) m/z [M + Na]$^+$ calculated: 1213.6857, found: 1213.6837. See Fig. S3† for HSQC NMR.

Synthesis of cyclo-[L-Trp-D-Leu-L-Lys(N$_3$)-D-Leu]$_2$ 10. The synthesis of cyclic peptide **10** has from linear peptide **4** using a similar protocol as described for the synthesis of cyclic peptide **9**. Details of the synthesis are described in Chapman et al.[37] ^{1}H NMR (500 MHz, TFA-d) δ ppm: 7.82 (d, 2H), 7.64 (d, 2H), 7.58 (s, 2H), 7.37–7.20 (m, 4H), 5.32 (t, 2H), 4.91 (t, 2H), 4.64–4.51 overlapping m, 4H), 3.41–3.06 (t, 4H), 2.0–0.6 (overlapping m, 48H). ^{13}C NMR (100 MHz, TFA-d) δ ppm: 174.9, 151.7, 136.9, 132.9, 129.8, 128.1, 124.5, 53.5, 52.1, 43.6, 37.9, 29.6, 28.7, 26.1, 25.8, 23.6, 22.4, 21.3, 21.1 (2 carbon signals obscured or overlapping). HRMS (MALDI-FTICR) m/z [M + Na]$^+$ calculated: 1155.6550, found: 1155.6533. See Fig. S4† for HSQC NMR.

Synthesis of cyclo-[L-Trp-D-Leu-L-Lys(Alloc)-D-Leu]$_2$ 11. DMTMM·BF$_4$ (80.5 mg, 0.245 mmol) was added to a solution of linear peptide **5** (300 mg, 0.204 mmol) in anhydrous DMF (41 mL, c = 0.005 M). The resulting mixture was stirred at ambient temperature for 3 d after which time the DMF was removed under reduced pressure. MeOH was then added to provide a suspension, which was subsequently cooled in an ice bath and then filtered under vacuum to collect the precipitate, which was washed with cold MeOH (10 mL). The filtrate was re-concentrated under reduced pressure, suspended in MeOH and filtered, each time colleting the precipitate. This process

was repeated until the filtrate was free of any precipitate. The combined precipitates were dried under high vacuum to provide the desired Boc-protected cyclic peptide (105 mg, 36%) as an off-white solid. ^{1}H NMR (400 MHz, TFA-d, with 10 equiv. LiBr) δ ppm: 8.14 (d, J = 8.2 Hz, 2H), 8.66 (d, J = 7.65 Hz, 2H), 7.57 (s, 2H), 7.40 (t, J = 7.4 Hz, 2H), 7.35 (t, J = 7.4 Hz), 5.94–5.84 (m, 2H), 5.33 (d, J = 17.2 Hz, 2H), 5.27 (d, J = 10.5 Hz, 2H), 5.23 (t, J = 7.3 Hz, 2H), 4.77 (t, J = 7.4 Hz, 2H), 4.75–4.63 (overlapping m, 8H), 3.37–3.29 (m, 4H), 3.24 (t, J = 6.7 Hz, 4H), 1.90–1.13 (overlapping m, 24H), 1.76 (s, 18H), 1.03–0.68 (overlapping m, 24H). HRMS (ESI+) m/z [M + Na]$^+$ calculated: 1471.8212, found: 1471.8206. The Boc-protecting groups were removed by treating the Boc-protected linear peptide with TFA/triisopropylsilane/thioanisole/water (85 : 5 : 5 : 5 v/v/v/v, 3 mL) for 3 h under an atmosphere of nitrogen. The reaction mixture was afterwards concentrated under reduced pressure and then triturated with cold diethylether to give **11** as an off-white solid in quantitative yield. HRMS (MALDI-FTICR) m/z [M + Na]$^+$ calculated: 1271.7163, found: 1271.7147. See Fig. S5† for HSQC NMR.

Synthesis of cyclo-[L-Lys(N$_3$)-D-Leu]$_4$ 12. The synthesis of cyclic peptide **12** has been described in Chapman et al.[38] ^{1}H NMR (500 MHz, TFA-d) δ ppm: 4.90–4.65 (m, 8H), 3.29 (t, J = 5.9 Hz, 8H), 2.15–1.13 (overlapping m, 40H), 1.06–0.70 (overlapping m, 24H). ^{13}C NMR (100 MHz, TFA-d) δ ppm 55.7, 54.8, 53.5, 45.2, 35.6, 30.0, 27.5, 25.0, 24.0, 23.9, 22.7, 22.6 (2 carbon signals obscured or overlapping). HRMS (MALDI-FTICR) m/z [M + Na]$^+$ calculated: 1091.6673, found: 1091.6654. See Fig. S6† for HSQC NMR.

Large unilamellar vesicle assays

Calcein- or 5(6)-carboxyfluorescein-entrapped LUVs consisting of either egg yolk phosphatidylcholine or *E. coli* total lipid extract were prepared *via* extrusion method as described in Danial et al.[41] Briefly, egg yolk phosphatidylcholine (10 mg) or *E. coli* total lipid extract (10 mg) was dissolved in chloroform (50 mL) after which slow removal of the solvent *via* rotary evaporation yielded a lipid film. The lipid film was then hydrated with a solution containing either calcein (40 mM) in sodium phosphate buffer (10 mM, pH 7.4) or 5(6)-carboxyfluorescein (30 μM) in sodium phosphate buffer (10 mM, pH 5.8) for 1–2 hours and placed in a sonic bath for 30 seconds. The suspension of lipid vesicles is then subjected to five freeze–thaw cycles followed by extrusion (29 times) through a 100 nm pore-size polycarbonate membrane using the Avanti® mini-extruder kit. The large unilamellar vesicles (LUVs) were then purified from unencapsulated fluorescent dye using a Sephadex G-200 column (25 cm × 4.0 cm) using phosphate buffer (10 mM, pH 7.4) in the case of calcein-entrapped LUVs and using phosphate buffer (10 mM, pH 5.8) in the case of 5(6)-carboxyfluorescein-entrapped LUVs. Elution of the calcein-entrapped LUVs was monitored visually through the appearance of a light yellow band from the column. Elution of the 5(6)-carboxyfluorescein-entrapped LUVs from the column was monitored using scattering of laser light observed by holding a hand-held laser pointer at the column nozzle. Both calcein- and 5(6)-carboxy-

This journal is © The Royal Society of Chemistry 2015

Org. Biomol. Chem., 2015, **13**, 2464–2473 | **2471**

fluorescein-entrapped LUVs were diluted in sodium phosphate buffer (10 mM, pH 7.4) to yield LUV solutions with a final lipid concentration 0.1 mg mL^{-1}. The size of the LUVs was verified using dynamic light scattering. All solutions containing LUVs were used in fluorescence experiments on the same day as preparation.

Time-dependent fluorescence was performed using a Perkin-Elmer LS50B luminescence spectrometer at 20 °C. Calcein or 5(6)-carboxyfluorescein-entrapped large unilamellar vesicles (2 mL, 0.1 mg mL^{-1}, 0.13 mM) were aliquoted into a disposable PMMA fluorescence cuvette. For the calcein-entrapped LUVs, the excitation wavelength was set at 493 nm and the emission wavelength was set at 505 nm, with excitation slit set at 2.5 nm and emission slit set at 10.0 nm. For the 5(6)-carboxyfluorescein-entrapped LUVs, the excitation wavelength was set at 493 nm and the emission wavelength was set at 510 nm, with the excitation slit set at 10.0 nm and the emission slit set at 15.0 nm. The emission of the baseline at 505 nm was monitored for ~50 seconds followed by the addition of the cyclic peptide (40 μL of 1 mM stock solution in DMSO). In a separate experiment, triton X-100 (40 μL, 10% w/v in 10 mM phosphate buffer, pH 7.4) was added to the cuvette containing LUVs to establish the maximum (calcein and 5(6)-carboxyfluorescein) fluorescence, f_T that can be attained in the assay. The change in 5(6)-carboxyfluorescein emission, Δf (in percent) was determined using the following equation:

$$\Delta f = \left[\frac{(f_s - f_b)}{(f_T - f_b)} \right] \times 100 \tag{1}$$

where f_s is the fluorescence signal at 280 seconds after addition of the sample, f_b is the fluorescence signal of the baseline before the addition of the sample at 40 seconds and f_T is the fluorescence signal after the addition of triton X-100.

Dynamic light scattering

Dynamic light scattering (DLS) measurements were performed on a Malvern ZetaSizer Nano S equipped with a 633 nm laser and a detector at 173° backscattering angle operating at 20 °C. Calcein-entrapped LUVs (2 mL, 0.1 mg mL^{-1}, 0.13 mM) made from egg yolk phosphatidylcholine or *E. coli* total lipid extract were aliquoted into a disposable PMMA fluorescence cuvette to which the cyclic peptide (40 μL of 1 mM stock solution in DMSO) was added. The samples were allowed to equilibrate for 10 minutes before the DLS measurement was initiated. Particle (CONTIN) size distributions were analyzed using the intensity distribution using the 'general purpose-normal resolution' mode in the Zetasizer software (v 6.32).

Notes and references

1 K. Murata, K. Mitsuoka, T. Hiral, T. Walz, P. Agre, J. B. Heymann, A. Engel and Y. Fujiyoshi, *Nature*, 2000, **407**, 599–605.
2 L. S. King, D. Kozono and P. Agre, *Nat. Rev. Mol. Cell Biol.*, 2004, **5**, 687–698.
3 D. A. Doyle, J. M. Cabral, R. A. Pfuetzner, A. Kuo, J. M. Gulbis, S. L. Cohen, B. T. Chait and R. MacKinnon, *Science*, 1998, **280**, 69–77.
4 R. Dutzler, E. B. Campbell, M. Cadene, B. T. Chait and R. MacKinnon, *Nature*, 2002, **415**, 287–294.
5 L. Song, M. R. Hobaugh, C. Shustak, S. Cheley, H. Bayley and J. E. Gouaux, *Science*, 1996, **274**, 1859–1866.
6 S. J. Singer and G. L. Nicolson, *Science*, 1972, **175**, 720–731.
7 S. Majd, E. C. Yusko, Y. N. Billeh, M. X. Macrae, J. Yang and M. Mayer, *Curr. Opin. Biotechnol.*, 2010, **21**, 439–476.
8 A. De La Escosura-Muñiz and A. Merkoçi, *ACS Nano*, 2012, **6**, 7556–7583.
9 B. A. Cornell, V. L. B. Braach-Maksvytis, L. G. King, P. D. J. Osman, B. Raguse, L. Wieczorek and R. J. Pace, *Nature*, 1997, **387**, 580–583.
10 J. J. Kasianowicz, E. Brandin, D. Branton and D. W. Deamer, *Proc. Natl. Acad. Sci. U. S. A.*, 1996, **93**, 13770–13773.
11 V. E. Carmichael, P. J. Dutton, T. M. Fyles, T. D. James, J. A. Swan and M. Zojaji, *J. Am. Chem. Soc.*, 1989, **111**, 767–769.
12 R. R. Ketchem, W. Hu and T. A. Cross, *Science*, 1993, **261**, 1457–1460.
13 M. R. Ghadiri, J. R. Granja and L. K. Buehler, *Nature*, 1994, **369**, 301–304.
14 A. J. Helsel, A. L. Brown, K. Yamato, W. Feng, L. Yuan, A. J. Clements, S. V. Harding, G. Szabo, Z. Shao and B. Gong, *J. Am. Chem. Soc.*, 2008, **130**, 15784–15785.
15 M. Langecker, V. Arnaut, T. G. Martin, J. List, S. Renner, M. Mayer, H. Dietz and F. C. Simmel, *Science*, 2012, **338**, 932–936.
16 J. R. Burns, E. Stulz and S. Howorka, *Nano Lett.*, 2013, **13**, 2351–2356.
17 N. Madhavan, E. C. Robert and M. S. Gin, *Angew. Chem., Int. Ed.*, 2005, **44**, 7584–7587.
18 N. Badi, L. Auvray and P. Guégan, *Adv. Mater.*, 2009, **21**, 4054–4057.
19 X. Zhou, G. Liu, K. Yamato, Y. Shen, R. Cheng, X. Wei, W. Bai, Y. Gao, H. Li, Y. Liu, F. Liu, D. M. Czajkowsky, J. Wang, M. J. Dabney, Z. Cai, J. Hu, F. V. Bright, L. He, X. C. Zeng, Z. Shao and B. Gong, *Nat. Commun.*, 2012, 3.

2472 | *Org. Biomol. Chem.*, 2015, **13**, 2464–2473

This journal is © The Royal Society of Chemistry 2015

20 L. Chen, W. Si, L. Zhang, G. Tang, Z. T. Li and J. L. Hou, *J. Am. Chem. Soc.*, 2013, **135**, 2152–2155.

21 W. Si, L. Chen, X. B. Hu, G. Tang, Z. Chen, J. L. Hou and Z. T. Li, *Angew. Chem., Int. Ed.*, 2011, **50**, 12564–12568.

22 T. M. Fyles, *Chem. Soc. Rev.*, 2007, **36**, 335–347.

23 S. Matile, A. Vargas Jentzsch, J. Montenegro and A. Fin, *Chem. Soc. Rev.*, 2011, **40**, 2453–2474.

24 B. Gong and Z. Shao, *Acc. Chem. Res.*, 2013, **46**, 2856–2866.

25 T. Liu, C. Bao, H. Wang, Y. Lin, H. Jia and L. Zhu, *Chem. Commun.*, 2013, **49**, 10311–10313.

26 R. Chapman, M. Danial, M. L. Koh, K. A. Jolliffe and S. Perrier, *Chem. Soc. Rev.*, 2012, **41**, 6023–6041.

27 J. Montenegro, M. R. Ghadiri and J. R. Granja, *Acc. Chem. Res.*, 2013, **46**, 2955–2965.

28 T. Suga, S. Osada and H. Kodama, *Bioorg. Med. Chem.*, 2012, **20**, 42–46.

29 S. Fernandez-Lopez, H. S. Kim, E. C. Choi, M. Delgado, J. R. Granja, A. Khasanov, K. Kraehenbuehl, G. Long, D. A. Weinberger, K. M. Wilcoxen and M. R. Ghadiri, *Nature*, 2001, **412**, 452–455.

30 J. R. Granja and M. R. Ghadiri, *J. Am. Chem. Soc.*, 1994, **116**, 10785–10786.

31 N. Khazanovich, J. R. Granja, D. E. McRee, R. A. Milligan and M. R. Ghadiri, *J. Am. Chem. Soc.*, 1994, **116**, 6011–6012.

32 J. Taira, S. Osada, R. Hayashi, T. Ueda, M. Jelokhani-Niaraki, H. Aoyagi and H. Kodama, *Bull. Chem. Soc. Jpn.*, 2010, **83**, 683–688.

33 J. Couet, J. D. Jeyaprakash, S. Samuel, A. Kopyshev, S. Santer and M. Biesalski, *Angew. Chem., Int. Ed.*, 2005, **44**, 3297–3301.

34 W. S. Horne, N. Ashkenasy and M. R. Ghadiri, *Chem. – Eur. J.*, 2005, **11**, 1137–1144.

35 M. G. J. ten Cate, N. Severin and H. G. Börner, *Macromolecules*, 2006, **39**, 7831–7838.

36 C. Reiriz, R. J. Brea, R. Arranz, J. L. Carrascosa, A. Garibotti, B. Manning, J. M. Valpuesta, R. Eritja, L. Castedo and J. R. Granja, *J. Am. Chem. Soc.*, 2009, **131**, 11335–11337.

37 R. Chapman, K. A. Jolliffe and S. Perrier, *Polym. Chem.*, 2011, **2**, 1956–1963.

38 R. Chapman, K. A. Jolliffe and S. Perrier, *Aust. J. Chem.*, 2010, **63**, 1169–1172.

39 L. Motiei, S. Rahimipour, D. A. Thayer, C.-H. Wong and M. R. Ghadiri, *Chem. Commun.*, 2009, 3693–3695.

40 M. Danial, C. M.-N. Tran, P. G. Young, S. Perrier and K. A. Jolliffe, *Nat. Commun.*, 2013, **4**, 2780.

41 M. Danial, C. M.-N. Tran, K. A. Jolliffe and S. Perrier, *J. Am. Chem. Soc.*, 2014, **136**, 8018–8026.

42 J. T. Fletcher, J. A. Finlay, M. E. Callow, J. A. Callow and M. R. Ghadiri, *Chem. – Eur. J.*, 2007, **13**, 4008–4013.

43 J. Sánchez-Quesada, H. S. Kim and M. R. Ghadiri, *Angew. Chem., Int. Ed.*, 2001, **40**, 2503–2506.

44 D. Wang, L. Guo, J. Zhang, R. W. Roeske, L. R. Jones, Z. Chen and C. Pritchard, *J. Pept. Res.*, 2001, **57**, 301–306.

45 T. D. Clark, L. K. Buehler and M. R. Ghadiri, *J. Am. Chem. Soc.*, 1998, **120**, 651–656.

46 R. García-Fandiño, M. Amorín, L. Castedo and J. R. Granja, *Chem. Sci.*, 2012, **3**, 3280–3285.

47 P. De Santis, S. Morosetti and R. Rizzo, *Macromolecules*, 1974, **7**, 52–58.

48 M. R. Ghadiri, J. R. Granja, R. A. Milligan, D. E. McRee and N. Khazanovich, *Nature*, 1993, **366**, 324–327.

49 S. L. Mellor, D. A. Wellings, J.-A. Fehrentz, M. Paris, J. Martinez, N. J. Ede, A. M. Bray, D. J. Evans and G. B. Bloomberg, in *Fmoc Solid Phase Peptide Synthesis*, Oxford Univ. Press, New York, NY, USA, 2000.

50 S. J. Butler and K. A. Jolliffe, *Org. Biomol. Chem.*, 2011, **9**, 3471–3483.

51 S. A. Raw, *Tetrahedron Lett.*, 2009, **50**, 946–948.

52 Y. Shai, *Biochim. Biophys. Acta, Biomembr.*, 1999, **1462**, 55–70.

53 A. V. Hill, *Biochem. J.*, 1913, **7**, 471–480.

54 Phospholipid compositions of Egg yolk phosphatidyl-choline and *E. coli* total lipid extract were derived from Avanti Polar lipids, Inc. http://www.avantilipids.com.

55 B. Kollmitzer, P. Heftberger, M. Rappolt and G. Pabst, *Soft Matter*, 2013, **9**, 10877–10884.

This journal is © The Royal Society of Chemistry 2015

Org. Biomol. Chem., 2015, **13**, 2464–2473 | **2473**